NOTE-GERBE-ALREADY / INTERPRETIVE THESIS AND CONDITIONAL THEOREM ARCHITECTURE

The Gerbe Was Already There

J. Scott Little

Source: v0.2.1, 3 August 2026 Publication treatment: 8 September 2026

Research notes — not peer reviewed. Trust, but verify. Always.

What higher-descent information is already present in familiar quantum-field structures?

A research note on higher descent, relative charge, and pair-only force, with a conditional confinement architecture and explicit bridge gates.

Scope and status

The final implication is conditional. The source does not claim the G1–G7 gates are all proved or establish unconditional confinement or a mass-gap theorem.

This edition adds a reading guide and publication notices. The source's mathematical status and historical provenance remain attached to its claims.

A way into the note

The central distinction

Projective implementation and coherent overlap phases can retain information that is absent from a single local observable presentation. Identifying that shape does not establish every proposed physical bridge.

A concrete example

If local implementers compose only up to a central phase on triple overlaps, record that phase and its coherence before trying to replace the system with one globally chosen representation.

What this approach gains

The note connects familiar charge and transport structures to a detailed sequence of witness obligations. It exposes the missing bridge between a structural detector and quantitative energetic statements.

Reading route

Start with the abstract and higher-descent interpretation. Then follow the VF8 theorem architecture alongside the G1–G7 witness worksheet.

Citation: J. Scott Little, The Gerbe Was Already There, v0.2.1, 3 August 2026; website production edition, 8 September 2026. Cite theorem and printed body-page numbers from the note itself.

The Gerbe Was Already There

A Research Note on Higher Descent, Relative Charge, and Pair-Only Force in Quantum Field Theory

Scott Little

Working Research Note RN-GQFT-01

Version 0.2.1 - 3 August 2026

Not peer reviewed. Trust, but verify. Always.

Abstract

This note advances an interpretive thesis rather than a priority claim: quantum field theory has carried gerbe-like structure from the beginning, even when the language of bundle gerbes, higher descent, and correspondence-valued gluing was not yet available. Projective implementation, charged superselection sectors, Wilson and 't Hooft operators, center-valued flux, Gauss-law boundary balance, local observables with globally nontrivial representation data, and composition preserved only up to coherent phase already exhibit the architecture later formalized by gerbes.

The note recasts those familiar structures in a positive-thickness Yang–Mills setting. It isolates a selected fixed-thickness $SU(3)$ branch with detector $I_3(\Omega_m) = \omega^m$ and then develops the full VF8.1–VF8.10 theorem architecture: detector-to-relative-flux realization, endpoint charge extraction, center-sensitive no-local-screening, finite-energy pair and transparent states, complete defect-channel coercivity, bounded-overlap bridge reconstruction, endpoint control, fixed-thickness lower tension, admissible thin transfer, and neutral finite-block homogenization.

The final implication is explicitly conditional. The note does not claim that the G1–G7 bridge gates are already proved, nor does it present an unconditional confinement or mass-gap theorem. Its contribution is to expose the hidden higher-descent shape, preserve the full proof architecture, and make every remaining verification obligation visible before memory and journal compression sand the interesting edges off it.

Editorial Statement

The phrase *the gerbe was already there* is not meant literally as a historical claim that early quantum field theory authors secretly used modern gerbe theory. It means something more modest and, in our view, more useful:

QFT repeatedly encountered the local data, projective composition, sector obstruction, and higher coherence that gerbes organize.

This note is therefore a recasting. The classical and quantum phenomena are not newly discovered here. What is new is the attempt to place them in one typed architecture and to use that architecture to formulate a concrete pair-only force and tension problem without pretending that the missing proofs have already volunteered for service.

NOT PEER REVIEWED. TRUST, BUT VERIFY. ALWAYS.

This document is a working research note. Conditional theorem schemas are not unconditional Yang–Mills results.

Contents

Part I - Interpretive and Structural Note

How familiar quantum-field-theoretic structures acquire a common higher-descent architecture.

1 The Gerbe Was Already There

1.1 The interpretive thesis

Quantum field theory has always lived with a mismatch between local description and global realization. Fields are written in charts, gauges, and local trivializations; physical observables are expected to be presentation independent; charged and vacuum sectors may fail to glue by literal equality; implementers may compose only projectively; and line operators may carry information invisible to strictly local adjoint observables.

Modern gerbe language does not create these facts. It provides a geometric and categorical home for them.

The note uses *gerbe-like* in a disciplined sense. A QFT structure is gerbe-like when the following pattern appears:

1. local objects exist on a cover;
2. overlap comparison data are noncanonical;
3. pairwise comparisons compose only up to coherent unitary, phase, line, or correspondence;
4. the resulting higher cocycle is invariant under allowed rephasings;
5. the ordinary observable shadow may glue strictly even while the represented or charged system remains twisted.

This pattern is already visible in several foundational QFT structures.

1.2 Projective implementation

Symmetries in quantum theory are frequently implemented projectively. Even when the observable automorphism is strict, the Hilbert-space implementer may be defined only up to phase. On triple compositions, the quotient between two parenthesized implementation routes is a cocycle. The familiar statement that rays, not vectors, are physical is therefore already a warning that representation data live one categorical level above ordinary observable composition.

A line bundle records phase ambiguity for single objects. A gerbe records coherent line ambiguity across overlap comparisons and triple compositions. The passage is not an aesthetic upgrade; it is the correct typing of repeated projective ambiguity.

1.3 Superselection sectors

Algebraic QFT separates the local observable net from its charged representations. A charge may be invisible in every sufficiently small neutral observable algebra while remaining globally detectable through representation class, transportability, conjugacy, or asymptotic flux.

That separation has the same formal shape used throughout this note:

$$\boxed{\text{strict observable shadow} \quad \text{with} \quad \text{nontrivial represented descent data.}}$$

The gerbe language becomes especially natural when no preferred global charged Hilbert bundle exists, but local charged realizations and their comparison correspondences do.

1.4 Wilson, 't Hooft, and extended operators

Wilson loops and 't Hooft operators already teach that the physically relevant gauge information is not exhausted by local field strength. Their algebra detects linked flux, center charge, and topological obstruction. Wilson's lattice construction made the surface content of confinement explicit, while the Hamiltonian formulation emphasized strings of electric flux that cannot end without charge. 't Hooft's operator algebra made the electric-magnetic and center-valued phase structure equally explicit.

The note does not claim that every Wilson or 't Hooft algebra *is* a bundle gerbe. It claims that once one asks how the local implementations, line operators, coefficient phases, and overlap comparisons glue, higher descent is already present.

1.5 Gauss law as a boundary law

Gauss law is not merely a differential equation in the interior. It is a relation between interior constraint and boundary charge. For discrete center flux, the relevant statement is exponentiated: the product of center detectors on oriented boundary components equals the interior source contribution.

In a source-free region,

$$\prod_a \mathsf{Z}(S_a)^{\epsilon_a} = \mathbf{1},$$

or, on simultaneous charge sectors,

$$\sum_a \epsilon_a q_a = 0 \quad \text{in } \mathbb{Z}_3.$$

This is the operator-algebraic shadow of the homological identity `boundary of boundary equals zero`.

1.6 What the note adds

The note adds neither Wilson loops nor projective sectors nor center flux. It adds a common architecture:

$$\boxed{\begin{array}{c}\text{coefficient detector} \longrightarrow \text{relative flux class} \longrightarrow \text{endpoint charge} \\ \longrightarrow \text{pair-only admissibility} \longrightarrow \text{relative force}\end{array}}$$

The value of the recasting is that each arrow becomes a separately auditable theorem obligation.

2 Retained Positive-Thickness `SU(3)` Input

2.1 Controlling source

The controlling retained source is the selected downstream closure of Paper III, version 1.8.0. It proves a complete positive-thickness realization on the selected source-free Sector-III `SU(3)` branch while explicitly withholding physical thin reconstruction, confinement, scattering, and mass-gap claims.

2.2 Fixed-thickness coefficient detector

For `m=1,2`, the selected fixed-thickness linked-flux class carries the detector

$$I_3(\Omega_m) = \omega^m \neq 1, \qquad \omega = e^{2\pi i/3}.$$

The detector is invariant under admissible normalized two-cochain rephasing because

$$I_3(\delta\lambda) = 1.$$

Thus the two nonzero orientations define inequivalent controlled fixed-thickness classes.

2.3 Strict observable shadow and twisted represented system

The ordinary physical observable assignment composes strictly. The represented chart-scale system remains correspondence valued and carries a nontrivial coefficient class. Scalar reassociators cancel from adjoint Ward functionals without becoming trivial in the represented Hilbert or correspondence system.

This distinction is central:

$$\boxed{\text{strict local observable composition} \not\Rightarrow \text{strict represented descent.}}$$

2.4 Complete-ground coercive profile

The retained closed positive-thickness form satisfies

$$\ker \overline{q}_x = \operatorname{Ran} P_{\Omega,x},$$

and

$$\overline{q}_x[\Psi] \geq \kappa_{\mathrm{cof}} \left\| (I - P_{\Omega,x})\Psi \right\|^2,$$

where

$$\kappa_{\mathrm{cof}} = \frac{1}{2}\left(\frac{17}{5} - \sqrt{\frac{557}{75}}\right) = 0.337404437602020\ldots > 0.337.$$

The profile is uniform on the declared margin-adapted positive-thickness family. It is not, by itself, a zero-thickness estimate.

2.5 Gauss-Ward and triality data

The retained branch supplies:

- bounded finite-stage interior Gauss generators;
- a gauge-invariant physical Hilbert space equal to their joint kernel;
- full finite Ward domains;
- collar Ward derivations;
- honest triality in the retained endpoint sectors;
- zero finite current defect;
- regional, chart, selected-Cauchy, and package-adapted transport compatibility.

2.6 Source-free branch firewall

The selected vacuum branch excludes primitive external collar, boundary, and worldsheet sources. The external Cartan-cap realization is retained only as a separate `YM + defect` comparison branch.

Source-freeness does not remove nonabelian self-interaction, center flux, coefficient twisting, or reassociators. It says that those structures must be carried by the Yang-Mills field and its physical descent data rather than deposited into an external defect module.

2.7 Scope

The retained results are powerful but do not yet provide:

- two separated endpoint charges;
- pair-only admissibility;
- a bridge thermodynamic family;
- a pair-versus-transparent energy theorem;
- a physical thin force or tension.

The remainder of the note begins at precisely that boundary.

3 From the Coefficient Gerbe to Relative Endpoint Charge

3.1 Separation and bridge geometry

Fix positive thickness `epsilon` and endpoint separation `R`. The symbol `R` is used deliberately because the retained manuscript uses `L_j` for a character cutoff.

Let

$$\mathcal{B}_{\varepsilon,R}$$

be an oriented resolved bridge with endpoint boundary

$$\partial\mathcal{B}_{\varepsilon,R} = \partial_-\mathcal{B}_{\varepsilon,R} \sqcup \partial_+\mathcal{B}_{\varepsilon,R}.$$

The center-flux carrier is assumed to retract, relative to its endpoints, to an oriented interval. Its selected longitudinal class is

$$[\mathcal{B}_{\varepsilon,R}] \in H_1\left(\mathcal{B}_{\varepsilon,R}, \partial\mathcal{B}_{\varepsilon,R}; \mathbb{Z}_3\right),$$

with

$$\partial_{\mathrm{rel}}[\mathcal{B}_{\varepsilon,R}] = [+] - [-].$$

3.2 Grade extraction

Define the detector-grade map

$$\vartheta([\Omega]) = m \quad \Longleftrightarrow \quad I_3(\Omega) = \omega^m.$$

On the selected cyclic subgroup, `vartheta` identifies the coefficient class with `Z_3`.

3.3 Meridional transgression

The physical linked-flux realization must identify the coefficient grade with a meridional triality character

$$\chi_m(a) = \omega^{ma}.$$

On a transverse disk `D_epsilon`, the meridional class transgresses to the transverse Thom class:

$$\delta_\perp[\chi_m] = m u_\varepsilon^\perp.$$

Poincare-Lefschetz duality sends the transverse Thom class to the oriented bridge spine:

$$\mathrm{PD}(u_\varepsilon^\perp) = [\mathcal{B}_{\varepsilon,R}].$$

Hence the realization map is

$$\boxed{\mathfrak{r}_{\varepsilon,R} = (\iota_{\mathcal{T}})_* \circ \mathrm{PD} \circ \delta_\perp \circ \chi \circ \vartheta.}$$

It satisfies

$$\boxed{\mathfrak{r}_{\varepsilon,R}([\widehat{\Omega}_m]_{\mathrm{phys}}) = m[\mathcal{B}_{\varepsilon,R}].}$$

3.4 Chain-level model

Choose an oriented longitudinal nerve spine

$$v_0 \xrightarrow{e_1} v_1 \xrightarrow{e_2} \cdots \xrightarrow{e_N} v_N.$$

The constant-grade chain is

$$c_{\varepsilon,R}(m) = m \sum_{j=1}^{N} e_j.$$

Its boundary telescopes:

$$\partial c_{\varepsilon,R}(m) = m(v_N - v_0).$$

Any variation of the grade between cells would produce interior boundary terms

$$(m_j - m_{j+1})v_j,$$

which are precisely internal screening endpoints or primitive defects. Longitudinal detector transport and source-freeness must exclude them.

3.5 Endpoint charges

Applying the relative boundary gives

$$\partial_{\mathrm{rel}}\mathfrak{r}_{\varepsilon,R}([\widehat{\Omega}_m]) = m[+] - m[-].$$

Writing this as

$$q_-[-] + q_+[+],$$

we obtain

$$\boxed{q_- = -m, \qquad q_+ = m.}$$

Thus

$$m = 1 \Longrightarrow (q_-, q_+) = (2, 1),$$

and

$$m = 2 \Longrightarrow (q_-, q_+) = (1, 2).$$

Total neutrality follows from the augmentation identity:

$$q_- + q_+ = 0.$$

3.6 The nonformal burden

The homological conclusion is formal once the following physical statements are proved:

1. the selected bridge carries the meridional character `chi_m`;
2. compressed meridional holonomy equals `omega^m` on every cross-section;
3. the detector is transported unchanged along the bridge;
4. no primitive source lies at an interior nerve vertex;
5. chart, Cauchy, refinement, and selected scale changes preserve the realization.

The coefficient class alone does not manufacture the spatial bridge.

4 Center-Sensitive Gauss Balance and No Local Screening

4.1 Infinitesimal and discrete constraints

The ordinary Gauss generators impose invariance under gauge transformations connected to the identity. A nontrivial `Z_3` sector can survive this constraint. Therefore

$$G(\lambda)\Psi = 0 \quad \forall\lambda$$

does not imply

$$q(\Psi) = 0 \quad \text{in } \mathbb{Z}_3.$$

The no-screening theorem requires an exponentiated center-sensitive boundary law.

4.2 Regional center detector

For an admitted linking representative `S`, introduce a unitary

$$\mathsf{Z}_{\varepsilon,R}(S)^3 = \mathbf{1}.$$

Its charge projectors are

$$P^q(S) = \frac{1}{3}\sum_{k=0}^{2} \omega^{-kq}\mathsf{Z}(S)^k.$$

A state in sector `q` satisfies

$$\mathsf{Z}(S)\Psi = \omega^q\Psi.$$

4.3 Exponentiated balance

For a source-free region with oriented center-sensitive boundary components `S_a`, require

$$\boxed{\prod_a \mathsf{Z}(S_a)^{\epsilon_a} = \mathbf{1}.}$$

On simultaneous charge sectors this is

$$\boxed{\sum_a \epsilon_a q_a = 0 \quad \text{in } \mathbb{Z}_3.}$$

This is the operator-algebraic realization of the relative-boundary identity.

4.4 Center neutrality of bounded local observables

Let

$$\mathcal{A}_{\varepsilon}^{\mathrm{vac}}(\mathcal{O})$$

be the bounded local source-free observable algebra. The decisive fixed-point statement is

$$\boxed{\alpha_k(A) = A \qquad \forall A \in \mathcal{A}_{\varepsilon}^{\mathrm{vac}}(\mathcal{O}).}$$

For a linking detector disjoint from the bounded dressing support,

$$[A, \mathsf{Z}(S)] = 0,$$

and therefore

$$[A, P^q(S)] = 0.$$

Every bounded local observable and every normal completely positive operation generated by such observables preserves the center-sector decomposition.

4.5 No-local-screening lemma

If a locally normal state obeys

$$\omega_q(P^q(S)) = 1,$$

then a bounded local dressing `A` produces

$$\omega_{q,A}(P^q(S)) = 1.$$

It cannot move the state to `q=0` when `q` is nonzero.

Thus local gluonic polarization can alter energy and field profile without changing triality.

4.6 One-endpoint contradiction

A bounded isolated endpoint region would contain a nonzero endpoint charge and no compensating bridge cut, asymptotic string, external matter, primitive defect, or charged boundary sector. The source-free center balance would require

$$q_{\pm} = 0,$$

contradicting

$$q_{\pm} = \pm m \neq 0.$$

Therefore a nontrivial endpoint cannot be a bounded isolated source-free vacuum object.

4.7 Allowed completions

A charged endpoint can be completed by:

- the opposite endpoint;
- a string or cone-localized dressing extending to infinity;
- matter of nonzero triality;
- a primitive external defect;
- a genuinely charged physical boundary sector.

Only the first lies in the selected bounded source-free pair comparison category.

4.8 Pair-only classification

If the neutral pair exists and the matched transparent reference exists, then

$$\boxed{\text{pair physical} + \text{transparent physical} + \text{isolated endpoints inadmissible} \Longrightarrow \text{Type C.}}$$

The correct connected force is therefore

$$F_{\varepsilon}^{\text{conn}}(R) = F_{\varepsilon}^{\text{pair}}(R) - F_{\varepsilon}^{0}(R).$$

5 Finite-Energy Pair and Matched Transparent Reference

5.1 Same habitat, different center realization

The pair and transparent branches are constructed on the same resolved incised region, with the same endpoint collar slots, bridge carrier, regional basis, selected Cauchy clock, local gauge complex, and renormalization prescription.

They differ in center-flux class:

$$\mathfrak{r}_{\varepsilon,R}^{\text{pair}} = m[\mathcal{B}_{\varepsilon,R}],$$

whereas

$$\mathfrak{r}_{\varepsilon,R}^{0} = 0.$$

The transparent reference does not fill the incision and does not import the external Cartan-cap branch.

5.2 Common observable shadow

The pair and transparent states are locally normal on the same ordinary observable shadow, or on canonically normally isomorphic regional shadows. Their global charged representations may remain inequivalent.

Thus the relative comparison is scalar:

$$E_\varepsilon^{\mathrm{rel}}(R) = E_\varepsilon^{\mathrm{pair}}(R) - E_\varepsilon^{0}(R),$$

not an operator subtraction on one Hilbert space.

5.3 Pair packet

The pair packet has the schematic correspondence composition

$$\mathfrak{P}_{\varepsilon,R}^{\mathrm{pair}} = \mathcal{E}_{\varepsilon,R}^{-m} \boxtimes \mathcal{E}_{\varepsilon,R}^{\mathrm{br},m} \boxtimes \mathcal{E}_{\varepsilon,R}^{m}.$$

The notation `boxtimes` records correspondence-valued composition rather than unrestricted tensor factorization.

The packet is globally neutral but locally nontransparent:

$$q_- + q_+ = 0, \qquad q_\pm \neq 0.$$

5.4 Pair-state construction routes

A finite-energy pair state may be obtained through any rigorously typed route:

1. a nonzero vector in the pair-sector form domain;
2. compression of a faithful finite-energy envelope state by the pair-sector projector;
3. a normal state induced from the pair-transparent linking correspondence;
4. a relative modular density supported in the pair sector.

The essential requirement is

$$P_{\varepsilon,R}^{\mathrm{pair}} \mathcal{D}(q_{\varepsilon,R}) \neq \{0\}.$$

5.5 Finite trial energy

A finite bridge at finite `R` contains finitely many cells. If the endpoint packets, each bridge cell, and each seam have finite energy, then a trial pair packet satisfies

$$E_\varepsilon^{\mathrm{trial}}(R) \le E_\varepsilon^{\mathrm{end},-} + E_\varepsilon^{\mathrm{end},+} + N(R)E_\varepsilon^{\mathrm{cell},m} + (N(R)-1)E_\varepsilon^{\mathrm{seam}} < \infty.$$

This proves nonemptiness of the finite-energy pair sector. It does not yet prove the optimal energy or tension.

5.6 Transparent state

The transparent state has neutral endpoint and bridge projectors, satisfies the same source-free Gauss-Ward conditions, and lies in the same local renormalization class.

Its selected vacuum energy may be shifted to zero:

$$\overline{q}_\varepsilon^0 = q_\varepsilon^0 - e_\varepsilon^0 \|\cdot\|^2.$$

The same scalar shift is applied to the pair branch.

5.7 Anchored interaction energy

At reference separation `R_*`, define

$$\boxed{\mathcal{V}_\varepsilon^{\mathrm{conn}}(R \mid R_*) = E_\varepsilon^{\mathrm{rel}}(R) - E_\varepsilon^{\mathrm{rel}}(R_*).}$$

Any separation-independent scalar normalization cancels.

5.8 Type-C existence theorem schema

At fixed positive thickness, Type C is closed once one proves:

- the detector-to-relative-flux map;
- center-sensitive no-local-screening;
- nonemptiness of the pair form domain;
- source-free Gauss-Ward compatibility of the pair;
- existence of the matched transparent state;
- common local-normal and renormalization class.

Then the one-endpoint subtraction terms are not merely unnecessary; they are ill typed because the corresponding vacuum objects do not exist.

6 Relative Force and Fixed-Thickness Tension Architecture

6.1 Force as a form derivative

For each branch `s` in `{pair,0}`, pull the physical Hamiltonian form at separation `R+h` back to a reference representation at `R` and define

$$\Phi^s_{\varepsilon,R} = -\left.\frac{d}{dh}\right|_{h=0} q^s_{\varepsilon,R}(h).$$

The force is the branchwise state expectation

$$F^s_\varepsilon(R) = \omega^s_{\varepsilon,R}\left(\Phi^s_{\varepsilon,R}\right).$$

The pair-connected force is

$$\boxed{F^{\mathrm{conn}}_\varepsilon(R) = F^{\mathrm{pair}}_\varepsilon(R) - F^0_\varepsilon(R).}$$

6.2 Pair-versus-transparent normalization

The subtraction must cancel:

- common ultraviolet counterterms;
- common neutral bulk density;
- common incision and collar background;

while preserving:

- the nontrivial center-sector spectral remainder;
- the connecting bridge energy;
- the transported complete-ground-complement coercivity.

A local counterterm may shift the Hamiltonian by a scalar local density. It may not subtract a nonlocal center-sector projector by hand.

6.3 Cellwise coercivity

Let `D_j` be the bridge-cell defect projector. The required witness-channel identification is

$$\widehat{K}_j \geq \nu_\varepsilon \kappa^{\mathrm{wit}}_\varepsilon D_j.$$

For exact nontrivial band occupancy,

$$\omega^{\mathrm{pair}}(D_j) = 1.$$

The retained positive-thickness constant gives a candidate

$$\kappa_\varepsilon^{\mathrm{wit}} = \kappa_{\mathrm{cof}} > 0.337,$$

once the new bridge projector is identified with the retained complete-ground complement.

6.4 Bounded-overlap reconstruction

Let `m_epsilon^star` bound the number of cell stars containing any positive local Hamiltonian term. A controlled reconstruction has the form

$$\widetilde{Q}_{\varepsilon,R}^{\mathrm{bridge}} \geq a_\varepsilon^{\mathrm{sum}} \sum_{j=1}^{N(R)} \widehat{K}_j - \mu_\varepsilon^{\mathrm{rec}} N(R) - C_\varepsilon^{\mathrm{end}}.$$

The normalized per-cell margin is

$$\boxed{\Delta_\varepsilon^{\mathrm{norm}} = a_\varepsilon^{\mathrm{sum}} \left(\nu_\varepsilon \eta_\varepsilon \kappa_\varepsilon^{\mathrm{wit}} - b_\varepsilon^{\mathrm{cell}}\right) - r_\varepsilon^{\mathrm{bulk}}.}$$

Fixed-thickness tension requires

$$\Delta_\varepsilon^{\mathrm{norm}} > 0.$$

6.5 Endpoint boundedness

The two physical endpoint stars must remain in a fixed controlled isomorphism class as `R` changes. Their total contribution must satisfy

$$|E_\varepsilon^{\mathrm{end}}(R)| \leq C_\varepsilon^{\mathrm{end}}$$

uniformly in `R`. Internal bridge seams are not endpoint terms; repeated seam loss belongs in the bulk reconstruction budget.

6.6 Energy-force identity

Under branchwise differentiability or a relative modular variational formula,

$$F_\varepsilon^{\mathrm{conn}}(R) = -\frac{d}{dR} E_\varepsilon^{\mathrm{rel}}(R).$$

Therefore

$$\mathcal{V}_\varepsilon^{\mathrm{conn}}(R \mid R_*) = -\int_{R_*}^{R} F_\varepsilon^{\mathrm{conn}}(r)\, dr.$$

6.7 Fixed-thickness lower tension

If

$$N(R) \geq \frac{R}{\ell_\varepsilon^+} - C_\varepsilon^N,$$

then

$$\mathcal{V}_\varepsilon^{\mathrm{conn}}(R \mid R_*) \geq \sigma_\varepsilon^{\mathrm{low}}(R - R_*) - C_{\varepsilon,R_*},$$

with

$$\boxed{\sigma_\varepsilon^{\mathrm{low}} = \frac{\Delta_\varepsilon^{\mathrm{norm}}}{\ell_\varepsilon^+} > 0.}$$

7 Thin Stability and the Thermodynamic Limit

7.1 Two limits

The note contains two distinct limits:

$$\varepsilon \downarrow 0$$

and

$$R \to \infty.$$

They may not be interchanged formally.

Fixed-`R` thin convergence constructs the thin pair-connected force and anchored energy. Large-`R` tension transfer requires a separate uniform thermodynamic theorem.

7.2 Admissible thin convergence

All thin limits are taken only along the selected cofinal thickness system and through the declared correspondences. No unrestricted convergence over arbitrary thickness sequences is asserted.

A typical form input is admissible Mosco convergence:

$$\widehat{q}^{s}_{\varepsilon,R} \xrightarrow{M} q^{s}_{0,R}, \qquad s \in \{\mathrm{pair}, 0\},$$

locally uniformly for `R` in compact intervals.

If the branchwise forces converge in local `L^1`, then

$$F^{\mathrm{conn}}_{\varepsilon} \to F^{\mathrm{conn}}_{0}$$

and

$$\mathcal{V}^{\mathrm{conn}}_{\varepsilon}(\cdot \mid R_*) \to \mathcal{V}^{\mathrm{conn}}_{0}(\cdot \mid R_*)$$

locally uniformly.

7.3 Uniform nondegeneration

The invariant thin quantity is the physical density

$$\frac{\Delta^{\mathrm{norm}}_{\varepsilon}}{\ell^{+}_{\varepsilon}},$$

not the raw per-cell gap.

A sufficient condition is

$$\inf_{\varepsilon<\varepsilon_0} \sigma^{\mathrm{low}}_{\varepsilon} \geq \sigma_* > 0.$$

This requires uniform control of:

- overlap multiplicity;
- witness-to-cell transport;
- defect occupancy;
- normalization loss;
- cell length;
- thin survival of the center detector.

7.4 Almost-additivity

Let

$$\mathscr{E}_{\varepsilon}(R) = E^{\mathrm{pair,rel}}_{\varepsilon}(R).$$

The central thermodynamic hypothesis is the uniform seam estimate

$$\boxed{|\mathscr{E}_\varepsilon(R_1 + R_2) - \mathscr{E}_\varepsilon(R_1) - \mathscr{E}_\varepsilon(R_2)| \le C_\#.}$$

The constant must be independent of the two lengths and of sufficiently small admissible thickness.

Together with a uniform linear trial upper bound, this gives the fixed-thickness thermodynamic density

$$\tau_\varepsilon = \lim_{R\to\infty} \frac{\mathscr{E}_\varepsilon(R)}{R}.$$

7.5 Uniform finite-block approximation

For a fixed block length `B`, almost-additivity gives

$$\left|\tau_\varepsilon - \frac{\mathscr{E}_\varepsilon(B)}{B}\right| \le \frac{C_{\mathrm{blk}}}{B},$$

uniformly in small admissible thickness.

At fixed `B`, admissible thin convergence gives

$$\mathscr{E}_\varepsilon(B) \to \mathscr{E}_0(B).$$

Taking first the thin limit at fixed block and then the large-block limit yields

$$\tau_\varepsilon \to \tau_0.$$

No direct exchange of `epsilon -> 0` and `R -> infinity` is used.

7.6 Thin tension theorem schema

If

$$\tau_\varepsilon \ge \sigma_* > 0$$

uniformly and the finite-block theorem holds, then

$$\boxed{\tau_0 = \lim_{R\to\infty} \frac{\mathcal{V}_0^{\mathrm{conn}}(R \mid R_*)}{R - R_*} \ge \sigma_* > 0.}$$

This remains conditional until the physical thin Yang-Mills form, no-leakage theorem, and uniform bridge concatenation are proved.

8 Theorem Ledger and Verification Gates

8.1 Status types

The note distinguishes:

- **R** - retained proved input;
- **C** - construction or theorem schema supplied by the note;
- **O** - open bridge-specific verification obligation;
- **T** - conditional theorem derived from retained inputs and verified hypotheses;
- **X** - explicit nonclaim.

8.2 Two different completion measures

Version 0.2.1 records two statuses that must not be confused.

1. **Architecture status:** VF8.1-VF8.10 now supply a complete conditional path through G1-G7.
2. **Verification status:** no gate is promoted to a proved bridge theorem merely because its theorem schema has been written.

The architecture is complete. The bridge verification remains open.

8.3 Retained inputs

The selected positive-thickness package supplies:

- the incised habitat and controlled regional basis;
- the source-free Sector-III branch;
- the nontrivial fixed-thickness detector for `m=1,2`;
- the strict ordinary observable shadow;
- correspondence-valued represented descent;
- honest triality and Gauss-Ward compatibility;
- the complete-ground projection;
- the uniform positive-thickness coercive constant.

8.4 VF8 technical architecture

The integrated Part II now contains:

- VF8.1 - detector-to-relative-flux realization;
- VF8.2 - center-sensitive Gauss balance and no local screening;
- VF8.3 - finite-energy pair and transparent state construction;
- VF8.4 - complete bridge-defect projector identification;
- VF8.5 - bounded-overlap global reconstruction;
- VF8.6 - uniform endpoint and cross-endpoint control;
- VF8.7 - fixed-thickness lower pair tension and force reconstruction;

- VF8.8 - uniform admissible thin-density transfer;
- VF8.9 - neutral finite-block almost-additivity and exact tension limit;
- VF8.10 - combined theorem, dependency graph, and claim-boundary audit.

8.5 G1-G7 gate status

Gate	Verification requirement	Architecture	Evidence
G1	Physical endpoint boundary map and opposite nonzero charges	VF8.1 complete	Open
G2	Pair-only admissibility and no bounded local dressing	VF8.2–VF8.3 complete	Open
G3	Complete bridge-cell defect-channel transport	VF8.4 complete	Open
G4	Positive normalized bounded-overlap margin	VF8.5 complete	Open
G5	Uniform $O(1)$ endpoint remainder	VF8.6 complete	Open
G6	Uniform physical thin density and nonrelaxation	VF8.8 complete	Open
G7	Uniform neutral finite-block almost-additivity	VF8.9 complete	Open

The earlier verification worksheet remains preserved in the package. An update at its end records the new theorem architecture without changing the evidence verdict.

8.6 Recommended proof order

$$\boxed{G1 \longrightarrow G2 \longrightarrow G3 \longrightarrow G5 \longrightarrow G4 \longrightarrow G6 \longrightarrow G7.}$$

The endpoint geometry and admissibility category must be fixed before the bridge energy is interpreted. The endpoint remainder is audited before finalizing the bulk margin so repeated seam losses cannot disappear into an `O(1)` box and hope nobody notices.

8.7 First unresolved theorem

The first genuinely new bridge theorem remains:

$$\boxed{\text{Endpoint Boundary Map and Pair-Only Admissibility Theorem.}}$$

It must prove that the retained coefficient class is physically realized by a relative bridge-flux class and that neither charged endpoint is independently physical in the selected source-free vacuum folium.

9 Nonclaims and Research-Note Boundary

9.1 No historical priority claim

The note does not claim that modern gerbe theory was literally formulated in the earliest QFT literature. It claims that QFT repeatedly displayed the structural phenomena that gerbes later organized.

9.2 No unconditional confinement theorem

The note does not yet prove confinement in four-dimensional pure Yang-Mills theory. It provides a conditional pair-tension architecture on the selected branch.

9.3 Topology is not energy

A nontrivial gerbe or endpoint class does not imply positive tension. Positive tension additionally requires:

- persistent realization in every bridge cell;
- complete defect-channel coercivity;
- bounded-overlap extensivity;
- positive normalization margin;
- endpoint control;
- thin nondegeneration.

9.4 Pair-only admissibility is not linear growth

A nonfactorizable pair may have bounded, logarithmic, sublinear, or linear energy. The energy law is analytic, not purely topological.

9.5 No isolated endpoint vacua

In the proposed Type-C category, isolated endpoint vacuum states are not introduced. A string to infinity, charged matter, external defect, or charged boundary belongs to a different comparison category.

9.6 No operator subtraction across inequivalent sectors

The relative quantities

$$E^{\mathrm{pair}} - E^{0}$$

and

$$F^{\mathrm{pair}} - F^{0}$$

are scalar comparisons after matched normalization. No global operator difference is assumed.

9.7 No hidden scale equivalence

General scale arrows remain correspondences or controlled isometries. They are not inverted unless an actual equivalence theorem exists.

9.8 No unrestricted thin limit

All thin statements are restricted to the selected admissible cofinal system.

9.9 No automatic mass-gap consequence

A positive pair tension would be an important confinement statement, but a vacuum spectral mass gap requires a separate no-leakage and spectral-transfer theorem.

9.10 Why this remains a note

The present work is best maintained as a research note because it:

- recasts known QFT structures in higher-descent language;
- preserves exploratory theorem architecture;
- records precise missing lemmas;
- provides historical and conceptual orientation;
- does not yet have the closed proof chain required of a journal theorem paper.

The note becomes a paper only after one or more of the currently open gates are independently closed and a genuinely new theorem is proved at the selected physical scope.

Part II - VF8 Technical Architecture

Detector realization, Type-C admissibility, coercive reconstruction, thin transfer, and finite-block homogenization.

10 VF8.1 - Detector-to-Relative-Flux Realization

10.1 Objective and claim boundary

Fix a selected positive thickness

$$\varepsilon \in E_{\mathrm{cof}},$$

an admissible endpoint separation `R`, and one of the retained nontrivial coefficient classes

$$[\widehat{\Omega}_m]_{\mathrm{phys}}, \qquad m \in \{1,2\}.$$

The retained calculation supplies

$$I_3(\widehat{\Omega}_m) = \omega^m, \qquad \omega = e^{2\pi i/3}.$$

The missing step is a physical realization map

$$\mathfrak{r}_{\varepsilon,R} : \langle [\widehat{\Omega}_1]_{\mathrm{phys}} \rangle \longrightarrow H_1(\mathcal{B}_{\varepsilon,R}, \partial\mathcal{B}_{\varepsilon,R}; \mathbb{Z}_3)$$

such that

$$\boxed{\mathfrak{r}_{\varepsilon,R}([\widehat{\Omega}_m]_{\mathrm{phys}}) = m[\mathcal{B}_{\varepsilon,R}].}$$

This map is not canonical from the abstract cohomology class alone. It becomes canonical only after fixing the selected physical linked-flux branch, a resolved tubular bridge, a bridge orientation, and the meridional triality convention. Otherwise we have merely noticed that two things are labeled by `Z_3` and congratulated ourselves too early.

10.2 Resolved tubular bridge

Let

$$\Theta_{\varepsilon,R} : [0,1] \times D_\varepsilon \longrightarrow \mathcal{T}_{\varepsilon,R} \subset \mathcal{B}_{\varepsilon,R}$$

be an admissible orientation-preserving tubular presentation. The parameter `s` increases from the negative endpoint to the positive endpoint. The horizontal boundary is

$$\partial_{\mathrm{h}}\mathcal{T}_{\varepsilon,R} = \mathcal{T}^-_{\varepsilon,R} \sqcup \mathcal{T}^+_{\varepsilon,R},$$

and the vertical boundary is

$$\partial_{\mathrm{v}}\mathcal{T}_{\varepsilon,R} = \Theta_{\varepsilon,R}([0,1]\times\partial D_\varepsilon).$$

A marked point in the transverse disk defines an oriented longitudinal spine

$$\gamma_{\varepsilon,R}(s) = \Theta_{\varepsilon,R}(s,p_\varepsilon).$$

Its image in relative homology is denoted

$$[\mathcal{B}_{\varepsilon,R}] \in H_1(\mathcal{B}_{\varepsilon,R},\partial\mathcal{B}_{\varepsilon,R};\mathbb{Z}_3).$$

The orientation convention is

$$\boxed{\partial_{\mathrm{rel}}[\mathcal{B}_{\varepsilon,R}] = [+]-[-].}$$

Here `[B]` is the relative longitudinal flux-spine class. It is not the ordinary fundamental class of the full higher-dimensional bridge region.

10.3 Algebraic grade extraction

Define

$$\vartheta([\Omega]) = m \quad\Longleftrightarrow\quad I_3(\Omega)=\omega^m.$$

Coboundary invariance of `I_3` makes `vartheta` independent of the normalized representative. On the selected cyclic subgroup,

$$\vartheta : \langle[\widehat{\Omega}_1]_{\mathrm{phys}}\rangle \xrightarrow{\cong} \mathbb{Z}_3.$$

The detector is multiplicative, hence

$$\vartheta([\Omega][\Omega']) = \vartheta([\Omega])+\vartheta([\Omega']) \quad \text{in } \mathbb{Z}_3.$$

This extracts the algebraic flux grade. It does not yet place that grade on a physical spatial carrier.

10.4 Chain-level insertion

Choose an ordered longitudinal spine in a marked bridge nerve,

$$v_0 \xrightarrow{e_1} v_1 \xrightarrow{e_2} \cdots \xrightarrow{e_N} v_N.$$

For `m in Z_3`, define

$$c_{\varepsilon,R}(m) = m \sum_{j=1}^{N} e_j.$$

Its boundary telescopes:

$$\partial c_{\varepsilon,R}(m) = m(v_N - v_0).$$

Thus it defines a relative class, and the oriented insertion map is

$$\iota^{\mathrm{br}}_{\varepsilon,R}(m) = [c_{\varepsilon,R}(m)] = m[\mathcal{B}_{\varepsilon,R}].$$

The formal marked realization is therefore

$$\mathfrak{r}_{\varepsilon,R} = \iota^{\mathrm{br}}_{\varepsilon,R} \circ \vartheta.$$

10.5 Meridional transgression

For each interior `s`, let

$$D_{\varepsilon,s} = \Theta_{\varepsilon,R}(\{s\} \times D_\varepsilon), \qquad \mu_{\varepsilon,s} = \partial D_{\varepsilon,s}.$$

The selected one-meridian carry is the triality character

$$\chi_m(a) = \omega^{ma}.$$

Under

$$\mathrm{Hom}(\mathbb{Z}_3, U(1)) \cong \mathbb{Z}_3,$$

this gives a meridional class in

$$H^1(\mu_{\varepsilon,s}; \mathbb{Z}_3).$$

The transverse connecting map sends it to the Thom class:

$$\delta_\perp[\chi_m] = m u^\perp_{\varepsilon,s}.$$

The family of transverse disks defines

$$u_\varepsilon^\perp \in H^2(\mathcal{T}_{\varepsilon,R}, \partial_{\mathrm{v}}\mathcal{T}_{\varepsilon,R}; \mathbb{Z}_3).$$

Poincare-Lefschetz duality gives

$$\mathrm{PD}_{\mathcal{T}}(u_\varepsilon^\perp) = [\gamma_{\varepsilon,R}].$$

Hence the physical realization formula is

$$\boxed{\mathfrak{r}_{\varepsilon,R} = (\iota_{\mathcal{T}})_* \circ \mathrm{PD}_{\mathcal{T}} \circ \delta_\perp \circ \chi \circ \vartheta.}$$

Schematically,

$$[\widehat{\Omega}_m] \xmapsto{I_3} m \xmapsto{\chi_m} m[\mu] \xmapsto{\delta_\perp} mu^\perp \xmapsto{\mathrm{PD}} m[\mathcal{B}].$$

10.6 Physical realization hypotheses

The homological formula becomes a physical theorem only after the following are verified.

RF1 - Meridional character. On every selected complete-ground transverse packet,

$$P_{\Omega,s}\,\mathrm{Hol}(\mu_{\varepsilon,s}) P_{\Omega,s} = \omega^m P_{\Omega,s}.$$

RF2 - Longitudinal constancy. Selected transport along the bridge intertwines the compressed meridional detector. A varying sequence of grades `m_j` would produce interior boundary terms

$$\sum_j (m_j - m_{j+1}) v_j,$$

which are additional screening defects or endpoints.

RF3 - No primitive interior source. No interior cell carries an external center source, charged matter insertion, or primitive defect current.

RF4 - Presentation naturality. Regional, chart, selected-Cauchy, refinement, and package-adapted scale comparisons preserve the detector grade, bridge orientation, and endpoint certificates. General scale correspondences are checked source and target separately; they are not inverted.

10.7 Theorem VF8.1

Assume RF1-RF4 and the resolved tubular bridge construction. Then

$$\boxed{\mathfrak{r}_{\varepsilon,R}([\widehat{\Omega}_m]_{\mathrm{phys}}) = m[\mathcal{B}_{\varepsilon,R}].}$$

Applying the relative boundary map gives

$$\partial_{\mathrm{rel}}\mathfrak{r}_{\varepsilon,R}([\widehat{\Omega}_m]) = m[+] - m[-].$$

Writing this boundary as

$$q_-[-] + q_+[+]$$

yields

$$\boxed{q_- = -m, \qquad q_+ = m.}$$

Thus

$$m = 1 \Longrightarrow (q_-, q_+) = (2, 1),$$

and

$$m = 2 \Longrightarrow (q_-, q_+) = (1, 2).$$

The pair is automatically neutral:

$$q_- + q_+ = 0.$$

10.8 Audit status

The algebraic detector and retained meridional triality data are available. The new unresolved work is the construction of the resolved two-endpoint bridge family and the verification that its local meridional detector is precisely the retained physical carry. Until that is done, $\mathtt{m}$ is a coefficient grade, not yet a certified ordered endpoint pair.

11 VF8.2 - Center-Sensitive Gauss Balance and No Local Screening

11.1 Ordinary Gauss law is not the whole story

Let

$$G_{\varepsilon,R}(\lambda)$$

be the retained infinitesimal Gauss generator for compactly supported

$$\lambda : \mathcal{O}_{\varepsilon,R} \to \mathfrak{su}(3).$$

Physical states satisfy

$$G_{\varepsilon,R}(\lambda)\Psi = 0.$$

This proves invariance under gauge transformations connected to the identity. It does not, by itself, determine a discrete center charge in

$$Z(SU(3)) \cong \mathbb{Z}_3.$$

Indeed, the retained branch simultaneously has vanishing infinitesimal Gauss defect and nontrivial triality. The center charge is a global or higher-form superselection datum, not a forgotten Lie-algebra charge.

11.2 Regional center detector

For every admitted linking representative S, require a unitary

$$\mathsf{Z}_{\varepsilon,R}(S), \qquad \mathsf{Z}_{\varepsilon,R}(S)^3 = I,$$

with spectrum contained in

$$\{1, \omega, \omega^2\}.$$

Define the charge projectors

$$\boxed{P^q_{\varepsilon,R}(S) = \frac{1}{3}\sum_{k=0}^{2} \omega^{-kq}\mathsf{Z}_{\varepsilon,R}(S)^k, \qquad q \in \mathbb{Z}_3.}$$

The detector must agree with the compressed meridional holonomy from VF8.1 and be natural under every admitted regional, chart, selected-Cauchy, refinement, and scale comparison.

11.3 Exponentiated center Gauss-Ward balance

Let a connected source-free testing region have oriented center-sensitive boundary components

$$S_1, \dots, S_r$$

with signs

$$\epsilon_a \in \{+1, -1\}.$$

The required source-free balance is

$$\boxed{\prod_{a=1}^{r} \mathsf{Z}(S_a)^{\epsilon_a} = I.}$$

On a simultaneous charge sector,

$$\mathsf{Z}(S_a)\Psi = \omega^{q_a}\Psi,$$

this becomes

$$\boxed{\sum_{a=1}^{r} \epsilon_a q_a = 0 \quad \text{in } \mathbb{Z}_3.}$$

With an external matter or defect charge `q_ext`, the right-hand side would be `-q_ext`. The selected vacuum branch imposes `q_ext=0`.

This multiplicative balance is the operator-algebraic form of the relative-chain identity that a source-free flux has no interior boundary.

11.4 Center neutrality of bounded local observables

Let

$$\mathcal{A}_{\varepsilon}^{\text{vac}}(\mathcal{O})$$

be the bounded source-free local observable algebra. The decisive fixed-point property is

$$\boxed{\alpha_k(A) = A \quad \forall A \in \mathcal{A}_{\varepsilon}^{\text{vac}}(\mathcal{O}), \quad k \in \mathbb{Z}_3.}$$

It excludes from the bounded local observable algebra:

- open fundamental Wilson lines with unpaired endpoints;
- primitive charged defects;
- nonzero-triality matter fields;
- semi-infinite strings extending to infinity.

For a detector `S` disjoint from the dressing support, locality and the fixed-point property imply

$$[A, \mathsf{Z}(S)] = 0,$$

and therefore

$$[A, P^q(S)] = 0.$$

A bounded local vacuum observable preserves every center-charge sector.

The same conclusion holds for normal completely positive operations generated by local Kraus operators, and for appropriately affiliated unbounded local fields whose domains are invariant under the sector projectors.

11.5 No-local-screening lemma

Let `omega_q` be a locally normal state satisfying

$$\omega_q(P^q(S)) = 1.$$

For a bounded local dressing `A`, define

$$\omega_{q,A}(B) = \frac{\omega_q(A^*BA)}{\omega_q(A^*A)}.$$

Since `A` commutes with `P^q(S)`,

$$\omega_{q,A}(P^q(S)) = 1.$$

Thus a bounded source-free local dressing cannot move a nontrivial endpoint into the neutral sector.

It may rearrange a gluonic polarization cloud. It may change the local energy. It may make the field profile look less rude. It cannot change the `Z_3` superselection charge.

11.6 One-endpoint region

Let `U^-` contain the negative endpoint and a finite initial bridge segment, but not the positive endpoint. Its center-sensitive boundary contains the endpoint detector `S_-` and an outgoing bridge cut `S_cut^-`. The source-free balance gives

$$q_- + q_{\text{cut}}^- = 0.$$

Since

$$q_- = -m,$$

we obtain

$$q_{\mathrm{cut}}^{-} = m.$$

The endpoint therefore requires outgoing nontrivial bridge flux. An analogous statement holds at the positive endpoint.

A bounded isolated endpoint state would have no outgoing bridge flux, no charge at infinity, no external matter, and no charged boundary absorber. The balance would force

$$q_{\pm} = 0,$$

contradicting VF8.1.

11.7 Permitted neutralizations outside the selected category

A nontrivial endpoint can be completed by:

1. the opposite endpoint;
2. a string or cone-localized dressing extending to infinity;
3. matter of nonzero triality;
4. a primitive external defect or Cartan cap;
5. a genuinely charged physical boundary sector.

Only the first is admitted in the selected bounded source-free vacuum comparison category.

11.8 Theorem VF8.2

Assume:

1. the endpoint charges from VF8.1 are nonzero;
2. regional center detectors exist and descend naturally;
3. the source-free exponentiated balance holds;
4. bounded local vacuum observables are center neutral;
5. primitive external sources and charged boundary absorbers are excluded;
6. strings to infinity are treated as different localization or asymptotic sectors.

Then neither endpoint can be screened by a bounded source-free local Yang-Mills dressing, and no bounded isolated endpoint state exists in the selected vacuum folium.

If a globally neutral pair state and a matched transparent state exist, the endpoint system is Type C.

11.9 Open obligations

The retained Gauss-Ward packet and honest triality strongly motivate the theorem, but the bridge note must still construct the actual regional detector operators, prove their exponentiated balance, and prove the fixed-point description of the selected bounded local observable algebra. Infinitesimal Gauss law alone is not allowed to impersonate all three statements.

12 VF8.3 - Finite-Energy Pair State and Matched Transparent Reference

12.1 Common resolved habitat

Fix positive thickness `epsilon` and finite separation `R`. The pair and transparent states are constructed on the same resolved incised region

$$\mathcal{O}_{\varepsilon,R} \Subset M \setminus \Sigma_{\mathrm{pres}},$$

with the same:

- endpoint collar stars;
- bridge carrier;
- exterior neighborhood;
- regional basis;
- selected Cauchy presentation;
- positive-thickness profile;
- local gauge complex;
- counterterm and seam prescription.

The pair carries the class

$$m[\mathcal{B}_{\varepsilon,R}],$$

while the transparent state carries the zero class. The transparent reference does not fill the incision or replace the source-free theory by the external Cartan-cap branch.

12.2 Common observable shadow, possibly inequivalent sectors

The pair and transparent states are locally normal on the same ordinary regional observable shadow, or on canonically normally isomorphic shadows. Their charged-sector representations may be globally inequivalent.

A common standard-form or linking-algebra comparison may be used, but no global unitary equivalence is required. The relative energy is a scalar comparison, not an operator subtraction across inequivalent Hilbert spaces.

12.3 Transparent reference

The transparent packet retains the full resolved geometry and source-free Gauss-Ward structure while assigning zero center flux:

$$\mathfrak{r}^0_{\varepsilon,R} = 0.$$

The endpoint detectors satisfy

$$\omega^0_{\varepsilon,R}(P^0(S_\pm)) = 1.$$

The preferred reference is the neutral complete-ground state when it exists. Let its branch energy be normalized by the same local scalar subtraction used in the pair branch.

12.4 Pair packet

Let

$$\mathcal{E}^{-m}_{\varepsilon,R}, \qquad \mathcal{E}^{\mathrm{br},m}_{\varepsilon,R}, \qquad \mathcal{E}^{m}_{\varepsilon,R}$$

be the endpoint and bridge correspondence packets. The complete pair packet is

$$\boxed{\mathfrak{P}^{\mathrm{pair}}_{\varepsilon,R} = \mathcal{E}^{-m}_{\varepsilon,R} \boxtimes \mathcal{E}^{\mathrm{br},m}_{\varepsilon,R} \boxtimes \mathcal{E}^{m}_{\varepsilon,R}.}$$

The symbol `boxtimes` denotes the selected correspondence composition, not an unrestricted tensor-product factorization.

The outer charges cancel:

$$-m + m = 0,$$

so the complete object is globally neutral while remaining locally nontransparent at the endpoint stars and bridge cross sections.

12.5 Source-free condition

The pair packet must introduce no primitive:

- collar source;
- worldsheet source;
- fundamental matter endpoint;
- defect current.

All collar data arise by restriction from the source-free interior field. The finite current defect remains zero.

12.6 Construction routes

Several equivalent realization routes may be available.

12.6.1 Finite-stage vector route

Choose a nonzero normalized vector

$$\Psi^{\mathrm{pair}}_{\varepsilon,R} \in P^{\mathrm{pair}}_{\varepsilon,R}\mathcal{D}(q_{\varepsilon,R})$$

and define the vector state. The decisive condition is

$$P^{\mathrm{pair}}_{\varepsilon,R}\mathcal{D}(q_{\varepsilon,R}) \neq \{0\}.$$

12.6.2 Normal-state compression route

Compress a faithful finite-energy envelope state by the pair-sector support projector and renormalize.

12.6.3 Correspondence-induced route

Use a positive functional on the linking algebra of the pair-versus-transparent correspondence. This is preferred when no strict common sector Hilbert space exists.

12.6.4 Relative modular route

Use a positive relative density affiliated with the appropriate linking or relative-commutant algebra and normalize it against the transparent state.

12.7 Pair-state conditions

The selected pair state must satisfy:

$$\omega^{\mathrm{pair}}_{\varepsilon,R}(P^{-m}(S_-)) = 1,$$

$$\omega^{\mathrm{pair}}_{\varepsilon,R}(P^{m}(S_+)) = 1,$$

and, for every interior bridge cross section,

$$\omega^{\mathrm{pair}}_{\varepsilon,R}(P^m(S_s)) = 1$$

in the exact route, or a uniform positive occupancy bound in the controlled route.

It must also satisfy:

- the ordinary Gauss kernel condition;
- the exponentiated center balance;
- the full Ward-domain condition;
- local normality on every admitted region;
- finite form energy at every finite `R`.

12.8 Finite-energy trial packet

A sufficient condition for pair-sector form-domain nonemptiness is a finite correspondence-composed trial packet built from:

1. finite-energy endpoint collar vectors;
2. finitely many nontrivial bridge-cell vectors;
3. neutral exterior complete-ground factors;
4. finitely many admissible seam correspondences.

For finite `R`, the number of cells is finite. If each endpoint, cell, and seam contribution has finite energy, then the complete trial packet has finite energy. This proves existence at fixed `R`; it does not yet prove the optimal asymptotic density.

12.9 Relative normalization

Define

$$E^{\mathrm{rel}}_{\varepsilon}(R) = E^{\mathrm{pair}}_{\varepsilon}(R) - E^{0}_{\varepsilon}(R).$$

The two branches must use identical:

- local counterterms;
- neutral bulk normalization;
- collar subtraction;
- time-translation normalization.

A safer anchored potential is

$$\mathcal{V}^{\mathrm{conn}}_{\varepsilon}(R \mid R_*) = E^{\mathrm{rel}}_{\varepsilon}(R) - E^{\mathrm{rel}}_{\varepsilon}(R_*),$$

which removes every `R`-independent scalar drift.

12.10 Theorem VF8.3

Assume the common habitat, source-free pair packet, pair-sector support, Gauss-Ward conditions, local normality, matched renormalization, and pair-sector form-domain nonemptiness. Then there exist finite-energy locally normal pair and transparent states for every finite admitted separation, and their scalar relative energy is well typed.

Combined with VF8.2, this closes the existence half of the Type-C theorem:

$$\boxed{\text{pair physical,}\quad \text{transparent physical,}\quad \text{isolated endpoints not physical.}}$$

12.11 Open obligations

The key new proof is not the formal correspondence product. It is the nonemptiness of the source-free pair form domain with the prescribed endpoint and bridge detector support, together with an honestly matched transparent state. Global neutrality is necessary. It is not a magical existence theorem.

13 VF8.4 - Bridge Defect Projector and the Complete-Ground Complement

13.1 Local bridge cells

Cover the interior bridge by uniformly controlled cells

$$\mathcal{B}^{(j)}_{\varepsilon,R}, \qquad j = 1, \ldots, N_\varepsilon(R).$$

Each cell carries:

- a transverse center detector `Z^(j)`;
- sector projectors `P^{q,(j)}`;
- a complete-ground projection `P_Omega^(j)`;
- a closed local form `qbar^(j)`.

For the oriented branch `m`, define the local bridge-defect projector

$$\boxed{D^{(j)}_{\varepsilon,R} = P^{m,(j)}_{\varepsilon,R}.}$$

The retained local estimate is

$$\overline{q}^{(j)}_{\varepsilon,R} \geq \kappa_{\mathrm{cof}}(I - P^{(j)}_{\Omega,\varepsilon,R}).$$

The missing analytic identification is

$$\boxed{D^{(j)}_{\varepsilon,R} \le I - P^{(j)}_{\Omega,\varepsilon,R}.}$$

13.2 Compatibility and ground neutrality

Require

$$[\mathsf{Z}^{(j)}, P^{(j)}_{\Omega}] = 0.$$

Then the local Hilbert packet decomposes simultaneously by center charge and complete-ground support.

The decisive neutrality statement is

$$\boxed{P^{(j)}_{\Omega} \le P^{0,(j)}.}$$

This says that the local zero-energy sector is transparent to the transverse bridge detector.

It does **not** say that the represented coefficient gerbe has become trivial on ground correspondences. The scalar reassociator may remain nontrivial in the represented comparison system while the local energy-ground vectors are neutral under the transverse charge detector. Those are different layers, and collapsing them would erase the very point of the note.

13.3 Exact projector theorem

Under detector-ground commutation and ground-sector neutrality,

$$P^{(j)}_{\Omega} P^{m,(j)} = 0 \quad (m \ne 0).$$

Hence

$$\boxed{D^{(j)} \le I - P^{(j)}_{\Omega}.}$$

The retained coercive bound then gives

$$\boxed{\overline{q}^{(j)} \ge \kappa_{\mathrm{cof}} D^{(j)}.}$$

If the pair state has exact local occupancy,

$$\omega^{\mathrm{pair}}(D^{(j)}) = 1,$$

then

$$\omega^{\mathrm{pair}}(\overline{q}^{(j)}) \geq \kappa_{\mathrm{cof}}.$$

More generally, if

$$\omega^{\mathrm{pair}}(D^{(j)}) \geq \eta_\varepsilon > 0,$$

then

$$\omega^{\mathrm{pair}}(\overline{q}^{(j)}) \geq \eta_\varepsilon \kappa_{\mathrm{cof}}.$$

13.4 Why one witness vector is not enough

A normalized vector of nontrivial triality with positive energy proves that one state costs energy. It does not prove that the entire physical defect channel is penalized.

If

$$D^{(j)}\mathcal{H} = \bigoplus_\alpha \mathcal{H}^{(j)}_{m,\alpha},$$

then every multiplicity channel `alpha` must be controlled. A rank-one witness that misses a low-energy multiplicity channel yields no uniform projector inequality.

13.5 Controlled correspondence route

Let

$$K^{\mathrm{wit}}_\varepsilon \geq \kappa^{\mathrm{wit}}_\varepsilon D^{\mathrm{wit}}_\varepsilon$$

be the retained finite witness packet. A normal correspondence or positive transport map must satisfy

$$\boxed{\rho^{(j)}_{\varepsilon,R}(D^{\mathrm{wit}}_\varepsilon) \geq \nu_\varepsilon D^{(j)}_{\varepsilon,R}, \qquad \nu_\varepsilon > 0.}$$

If the physical cell form obeys

$$\overline{q}^{(j)}_{\varepsilon,R} \geq a^{\mathrm{cell}}_\varepsilon \rho^{(j)}_{\varepsilon,R}(K^{\mathrm{wit}}_\varepsilon) - b^{\mathrm{cell}}_\varepsilon I,$$

then

$$\boxed{\overline{q}^{(j)}_{\varepsilon,R} \geq a^{\mathrm{cell}}_\varepsilon \nu_\varepsilon \kappa^{\mathrm{wit}}_\varepsilon D^{(j)}_{\varepsilon,R} - b^{\mathrm{cell}}_\varepsilon I.}$$

This formulation respects noninvertible scale and regional correspondences. Source and target certificates are proved in their own fibers.

13.6 Uniformity

The constants

$$\nu_\varepsilon, \quad a_\varepsilon^{\text{cell}}, \quad b_\varepsilon^{\text{cell}}, \quad \eta_\varepsilon$$

must be independent of the interior cell index and the total separation `R`. Endpoint cells are excluded from the uniform bulk family and handled separately.

13.7 Theorem VF8.4

Assume the bridge detector is well defined, the complete-ground projector commutes with it, the complete-ground sector is center neutral, the full nontrivial multiplicity channel is covered, and the pair state has uniform defect occupancy. Then the complete bridge-defect channel lies in the retained coercive complement and pays a uniform positive local energy cost.

13.8 Open obligations

The retained manuscript supplies the complete-ground projection, its kernel theorem, the positive gap, and the transport architecture. The genuinely new work is to prove that the new transverse bridge detector is the retained physical detector, that the local complete-ground sector is transparent to it, and that no nontrivial multiplicity channel escapes the witness comparison.

14 VF8.5 - Bounded-Overlap Reconstruction of the Global Bridge Bound

14.1 What is being counted

The global relative class

$$m[\mathcal{B}_{\varepsilon,R}]$$

is one topological object. The proof does not count it `N(R)` times and call that energy.

Instead:

1. the global class forces the same nontrivial detector grade through every transverse cell;
2. each cell has a distinct positive local Hamiltonian contribution;

3. a bounded-overlap theorem controls how often each Hamiltonian term enters the localization sum.

Topology supplies persistence. Locality supplies extensivity.

14.2 Positive local core

Let the positive bridge core form be

$$Q^{\mathrm{core}}_{\varepsilon,R} = \sum_{X\in\mathfrak{X}_{\varepsilon,R}} h_{\varepsilon,X}, \qquad h_{\varepsilon,X} \geq 0.$$

For each enlarged cell star define

$$Q^{\mathrm{core},(j)}_{\varepsilon,R} = \sum_{X\subset \mathrm{St}^{(j)}} w_{j,X} h_{\varepsilon,X}, \qquad 0 \leq w_{j,X} \leq 1.$$

Assume every local term appears in at most

$$m^{\star}_{\varepsilon} < \infty$$

cell stars. Then

$$\sum_j Q^{\mathrm{core},(j)}_{\varepsilon,R} \leq m^{\star}_{\varepsilon} Q^{\mathrm{core}}_{\varepsilon,R},$$

so

$$\boxed{Q^{\mathrm{core}}_{\varepsilon,R} \geq \frac{1}{m^{\star}_{\varepsilon}} \sum_j Q^{\mathrm{core},(j)}_{\varepsilon,R}.}$$

14.3 Pair-versus-transparent normalization

Subtract the matched transparent neutral cell and seam density as a scalar inside the pair branch. Let

$$\widetilde{Q}^{\mathrm{bridge}}_{\varepsilon,R}$$

denote the resulting shifted pair form.

Require a global physical-to-core estimate

$$\boxed{\widetilde{Q}^{\mathrm{bridge}}_{\varepsilon,R} \geq a^{\mathrm{glob}}_{\varepsilon} Q^{\mathrm{core}}_{\varepsilon,R} - r^{\mathrm{bulk}}_{\varepsilon} N_{\varepsilon}(R) I - C^{\mathrm{end}}_{\varepsilon} I.}$$

The repeated bulk loss `r_bulk N(R)` includes every IMS, seam, quasilocal-tail, and form-comparison error occurring once per cell. It may not be hidden in an `O(1)` endpoint constant.

14.4 Cell-to-witness comparison

Assume

$$Q^{\mathrm{core},(j)}_{\varepsilon,R} \geq \frac{1}{A^{\mathrm{cell}}_{\varepsilon}} \widehat{K}^{(j)}_{\varepsilon,R}.$$

Define

$$\boxed{a^{\mathrm{sum}}_{\varepsilon} = \frac{a^{\mathrm{glob}}_{\varepsilon}}{A^{\mathrm{cell}}_{\varepsilon} m^{\star}_{\varepsilon}}.}$$

Then

$$\widetilde{Q}^{\mathrm{bridge}}_{\varepsilon,R} \geq a^{\mathrm{sum}}_{\varepsilon} \sum_{j=1}^{N_{\varepsilon}(R)} \widehat{K}^{(j)}_{\varepsilon,R} - r^{\mathrm{bulk}}_{\varepsilon} N_{\varepsilon}(R) I - C^{\mathrm{end}}_{\varepsilon} I.$$

14.5 Insert the local defect theorem

Using the controlled VF8.4 estimate,

$$\widehat{K}^{(j)}_{\varepsilon,R} \geq \nu_{\varepsilon} \kappa^{\mathrm{wit}}_{\varepsilon} D^{(j)}_{\varepsilon,R} - b^{\mathrm{cell}}_{\varepsilon} I.$$

If

$$\omega^{\mathrm{pair}}_{\varepsilon,R}(D^{(j)}_{\varepsilon,R}) \geq \eta_{\varepsilon} > 0,$$

then

$$E^{\mathrm{bridge,rel}}_{\varepsilon}(R) \geq \Delta^{\mathrm{norm}}_{\varepsilon} N_{\varepsilon}(R) - C^{\mathrm{end}}_{\varepsilon},$$

where

$$\boxed{\Delta^{\mathrm{norm}}_{\varepsilon} = a^{\mathrm{sum}}_{\varepsilon} \left(\nu_{\varepsilon} \eta_{\varepsilon} \kappa^{\mathrm{wit}}_{\varepsilon} - b^{\mathrm{cell}}_{\varepsilon} \right) - r^{\mathrm{bulk}}_{\varepsilon}.}$$

14.6 Effective threshold and the selected witness

Define

$$\rho_\varepsilon = \frac{b_\varepsilon^{\mathrm{cell}} + r_\varepsilon^{\mathrm{bulk}}/a_\varepsilon^{\mathrm{sum}}}{\nu_\varepsilon \eta_\varepsilon}.$$

Then

$$\Delta_\varepsilon^{\mathrm{norm}} = a_\varepsilon^{\mathrm{sum}} \nu_\varepsilon \eta_\varepsilon (\kappa_\varepsilon^{\mathrm{wit}} - \rho_\varepsilon).$$

For the selected two-sector comparison matrix,

$$\kappa_\varepsilon^{\mathrm{wit}} = \frac{c_{\mathrm{UV}} + c_{\mathrm{IR}}}{2} - \frac{1}{2}\sqrt{(c_{\mathrm{UV}} - c_{\mathrm{IR}})^2 + 4\varepsilon_{\mathrm{mix}}^2}.$$

The reconstructed margin is positive precisely when the shifted matrix is positive:

$$\rho_\varepsilon < \min\{c_{\mathrm{UV}}, c_{\mathrm{IR}}\},$$

and

$$\boxed{\varepsilon_{\mathrm{mix}}^2 < (c_{\mathrm{UV}} - \rho_\varepsilon)(c_{\mathrm{IR}} - \rho_\varepsilon).}$$

14.7 Physical length

If interior cell lengths satisfy

$$0 < \ell_\varepsilon^- \le \ell_{\varepsilon,j} \le \ell_\varepsilon^+ < \infty,$$

then

$$N_\varepsilon(R) \ge \frac{R}{\ell_\varepsilon^+} - c_\varepsilon^{\mathrm{geom}}.$$

Define

$$\boxed{\sigma_\varepsilon^{\mathrm{low}} = \frac{\Delta_\varepsilon^{\mathrm{norm}}}{\ell_\varepsilon^+}.}$$

If `Delta_norm > 0`,

$$E_\varepsilon^{\mathrm{bridge,rel}}(R) \ge \sigma_\varepsilon^{\mathrm{low}} R - C_\varepsilon^{\mathrm{bridge}}.$$

14.8 Exact stationary specialization

In the exact route,

$$a_\varepsilon^{\mathrm{glob}} = A_\varepsilon^{\mathrm{cell}} = \nu_\varepsilon = \eta_\varepsilon = 1,$$

and

$$b_\varepsilon^{\mathrm{cell}} = r_\varepsilon^{\mathrm{bulk}} = 0.$$

Then

$$\Delta_\varepsilon^{\mathrm{norm}} = \frac{\kappa_{\mathrm{cof}}}{m_\varepsilon^\star},$$

and

$$\sigma_\varepsilon^{\mathrm{low}} = \frac{\kappa_{\mathrm{cof}}}{m_\varepsilon^\star \ell_\varepsilon^+}.$$

14.9 Theorem VF8.5

Assume a positive local-core decomposition, finite incidence multiplicity, uniform cell-to-witness comparison, complete defect-channel control, persistent occupancy, and a complete ledger of all repeated bulk losses. If

$$\Delta_\varepsilon^{\mathrm{norm}} > 0,$$

then the bridge-relative energy has a positive lower density proportional to physical separation.

14.10 Open obligations

The actual support geometry must be used to compute `m_star`, the cell-length calibration, and every seam/localization loss. “Finite overlap” is not a number, and a theorem that needs the number does not accept vibes as a substitute.

15 VF8.6 - Uniform Endpoint Remainder and Cross-Endpoint Control

15.1 Allowed `O(1)` terms

After the interior bridge reconstruction, the only terms permitted in the endpoint remainder are:

1. the negative endpoint star;
2. the positive endpoint star;
3. the two endpoint-to-bridge attachment seams;
4. a genuine direct cross-endpoint interaction;
5. a fixed exterior or anchoring correction.

Repeated interior seams remain in the bulk margin from VF8.5.

Write

$$E_\varepsilon^{\mathrm{rel}}(R) = E_\varepsilon^{\mathrm{bridge,rel}}(R) + \mathcal{R}_\varepsilon^{\mathrm{end}}(R).$$

The target is

$$\boxed{|\mathcal{R}_\varepsilon^{\mathrm{end}}(R)| \le C_\varepsilon^{\mathrm{end}}}$$

with a constant independent of `R`.

15.2 Rigid endpoint stars

Choose endpoint stars

$$\mathrm{St}^-_{\varepsilon,R}, \qquad \mathrm{St}^+_{\varepsilon,R}$$

of uniformly bounded diameter. Each contains the endpoint collar, detector, a fixed bridge segment, all local interactions touching the endpoint, and exactly one attachment seam.

Require selected transports from fixed model endpoint packets to the endpoint packets at separation `R`. These transports preserve:

- endpoint charge projectors;
- complete-ground support;
- local Gauss-Ward data;
- form domains;
- collar orientation;
- renormalization convention.

They may be correspondences or isometries. The global pair representations need not be equivalent.

15.3 Uniform endpoint form bounds

Let

$$e^s_{\varepsilon,\pm}(R) = \omega^s_{\varepsilon,R}(Q^{s,\pm}_{\varepsilon,R}), \qquad s \in \{\mathrm{pair}, 0\}.$$

Require

$$|e^s_{\varepsilon,\pm}(R)| \leq C^s_{\varepsilon,\pm}$$

uniformly in `R`. Exact rigid transport may make these expectations constant, but uniform form boundedness is sufficient.

Rigid support geometry alone does not prove a uniformly bounded expectation in a changing entangled global state. The local state family still needs form control.

15.4 Attachment seams

There are exactly two attachment seams. Their pair and transparent expectations must satisfy uniform bounds. The sum of all internal seams is excluded from this category, even if each individual seam is harmless. A thousand harmless constants remain a thousand constants.

15.5 Direct cross-endpoint interaction

Let

$$Q^{s,\mathrm{cross}}_{\varepsilon,R}$$

collect Hamiltonian terms whose support meets both endpoint stars.

15.5.1 Finite-range route

If the interaction range is `r_int`, then for sufficiently large separation the endpoint stars are farther apart than `r_int`, and

$$Q^{s,\mathrm{cross}}_{\varepsilon,R} = 0.$$

15.5.2 Quasilocal route

If interaction tails obey a summable bound `F_epsilon(r)` with `F_epsilon(r) -> 0`, require

$$\|Q^{s,\mathrm{cross}}_{\varepsilon,R}\| \leq C^{\mathrm{geom}}_{\varepsilon} F_\varepsilon(d^{-+}_{\varepsilon,R}).$$

Then the direct cross-endpoint scalar is uniformly bounded and typically decays to zero.

Long-range state correlations do not themselves constitute a direct Hamiltonian term. Factorization is not required merely to prove an `O(1)` endpoint energy.

15.6 Exterior matching

The pair and transparent states share the same exterior incised habitat, local counterterms, and selected clock. Any residual exterior scalar must vanish or remain uniformly bounded.

15.7 Theorem VF8.6

Assume rigid endpoint geometry, uniform endpoint form bounds, uniform control of the two attachment seams, finite-range or summable quasilocal cross-endpoint interactions, matched exterior normalization, and a clean firewall keeping repeated internal seams in the bulk ledger. Then

$$\boxed{|\mathcal{R}_\varepsilon^{\mathrm{end}}(R)| \le C_\varepsilon^{\mathrm{end}}.}$$

Combining with VF8.5 gives

$$\boxed{E_\varepsilon^{\mathrm{rel}}(R) \ge \Delta_\varepsilon^{\mathrm{norm}} N_\varepsilon(R) - C_\varepsilon^{\mathrm{tot}},}$$

and therefore

$$E_\varepsilon^{\mathrm{rel}}(R) \ge \sigma_\varepsilon^{\mathrm{low}} R - C_\varepsilon^{\mathrm{tot}}.$$

15.8 Force-level warning

An `O(1)` energy remainder does not imply that its derivative tends to zero. A bounded function may oscillate violently. Pointwise endpoint-force decay requires additional absolute-continuity and derivative-tail estimates.

15.9 Thin-transfer warning

For fixed thickness it is enough that

$$C_\varepsilon^{\mathrm{end}} < \infty.$$

Thin transfer requires the stronger uniform estimate

$$\sup_{\varepsilon \in E_{\mathrm{tail}}} C_\varepsilon^{\mathrm{end}} < \infty.$$

16 VF8.7 - Fixed-Thickness Pair-Tension Theorem and Force Reconstruction

16.1 Combine G1-G5

Assume the following have been verified at fixed positive thickness:

- **G1:** endpoint charges `q_-=-m`, `q_+=m`;
- **G2:** pair-only Type-C admissibility;
- **G3:** complete bridge-defect control;
- **G4:** positive normalized reconstruction margin;
- **G5:** uniform `O(1)` endpoint remainder.

Then

$$\boxed{E_\varepsilon^{\mathrm{rel}}(R) \geq \Delta_\varepsilon^{\mathrm{norm}} N_\varepsilon(R) - C_\varepsilon^{\mathrm{tot}}.}$$

Using the cell-count geometry,

$$\boxed{E_\varepsilon^{\mathrm{rel}}(R) \geq \sigma_\varepsilon^{\mathrm{low}} R - \widetilde{C}_\varepsilon^{\mathrm{tot}},}$$

where

$$\sigma_\varepsilon^{\mathrm{low}} = \frac{\Delta_\varepsilon^{\mathrm{norm}}}{\ell_\varepsilon^{+}} > 0.$$

16.2 Lower fixed-thickness pair tension

Define

$$\boxed{\underline{\sigma}_\varepsilon = \liminf_{R\to\infty} \frac{E_\varepsilon^{\mathrm{rel}}(R)}{R}.}$$

Then

$$\boxed{\underline{\sigma}_\varepsilon \geq \sigma_\varepsilon^{\mathrm{low}} > 0.}$$

This is the strongest conclusion available without a finite-block theorem.

16.3 Anchored potential

For fixed reference separation `R_*`, define

$$\mathcal{V}_\varepsilon^{\mathrm{conn}}(R \mid R_*) = E_\varepsilon^{\mathrm{rel}}(R) - E_\varepsilon^{\mathrm{rel}}(R_*).$$

Then

$$\liminf_{R\to\infty} \frac{\mathcal{V}_\varepsilon^{\mathrm{conn}}(R \mid R_*)}{R - R_*} \geq \sigma_\varepsilon^{\mathrm{low}}.$$

The anchored form removes every `R`-independent scalar ambiguity.

16.4 Mechanical force and restoring tension

When the branchwise scalar energies are differentiable, define

$$F_\varepsilon^s(R) = -\frac{d}{dR} E_\varepsilon^s(R), \qquad s \in \{\mathrm{pair}, 0\}.$$

The connected mechanical force is

$$F_\varepsilon^{\mathrm{conn}}(R) = F_\varepsilon^{\mathrm{pair}}(R) - F_\varepsilon^0(R) = -\frac{d}{dR} E_\varepsilon^{\mathrm{rel}}(R).$$

Define the positive restoring tension by

$$\boxed{\mathcal{T}_\varepsilon^{\mathrm{conn}}(R) = -F_\varepsilon^{\mathrm{conn}}(R) = \frac{d}{dR} E_\varepsilon^{\mathrm{rel}}(R).}$$

An attractive mechanical force is negative in the outward `R` direction; the restoring tension is positive.

16.5 Branchwise differentiation

The pair and transparent derivatives are taken in their own representations using branchwise displacement transport. No operator subtraction across sectors is needed.

For differentiable stationary minimizers, an appropriate form-level Hellmann-Feynman theorem gives

$$\frac{d}{dR} E_\varepsilon^s(R) = \omega_{\varepsilon,R}^s(\partial_R H_{\varepsilon,R}^s).$$

For a general changing state family, an additional state-variation term appears and may not be dropped.

16.6 Finite differences and Cesaro force

Without pointwise differentiability, define

$$\mathcal{T}^{\mathrm{conn}}_{\varepsilon,h}(R) = \frac{E^{\mathrm{rel}}_{\varepsilon}(R+h) - E^{\mathrm{rel}}_{\varepsilon}(R)}{h}.$$

If the relative energy is absolutely continuous,

$$E^{\mathrm{rel}}_{\varepsilon}(R) - E^{\mathrm{rel}}_{\varepsilon}(R_*) = \int_{R_*}^{R} \mathcal{T}^{\mathrm{conn}}_{\varepsilon}(s)\, ds.$$

Therefore,

$$\boxed{\liminf_{R\to\infty} \frac{1}{R-R_*} \int_{R_*}^{R} \mathcal{T}^{\mathrm{conn}}_{\varepsilon}(s)\, ds \geq \sigma^{\mathrm{low}}_{\varepsilon}.}$$

This is the legitimate force consequence of the linear lower energy bound.

16.7 What does not follow

The inequality

$$E(R) \geq \sigma R - C$$

does not imply

$$E'(R) \geq \sigma$$

pointwise. It also does not imply that `E(R)/R` has a limit. Bounded or sublinear oscillations may remain.

An optional linear trial-state upper bound gives a finite interval between the lower and upper asymptotic densities, but an almost-additivity theorem is still required to prove equality.

16.8 Theorem VF8.7

Under G1-G5, the selected Type-C pair has a strictly positive lower asymptotic energy density at fixed positive thickness. If the energy is absolutely continuous, its restoring tension has a strictly positive lower Cesaro average.

This is not yet a thin tension, a pointwise force limit, or a mass-gap theorem.

17 VF8.8 - Uniform Thin-Density Transfer

17.1 The actual uniform quantity

At each positive thickness,

$$\sigma_\varepsilon^{\mathrm{low}} = \frac{a_\varepsilon^{\mathrm{sum}}(\nu_\varepsilon \eta_\varepsilon \kappa_\varepsilon^{\mathrm{wit}} - b_\varepsilon^{\mathrm{cell}}) - r_\varepsilon^{\mathrm{bulk}}}{\ell_\varepsilon^+}.$$

A uniform lower bound on `kappa_epsilon` alone is not a uniform tension theorem. Every geometric and reconstruction factor must survive.

17.2 Uniform positive-thickness hypotheses

Choose an admissible cofinal sequence

$$\varepsilon_n \downarrow 0.$$

Require a cofinal tail on which:

UT1 - Uniform reconstructed density. There is `sigma_* > 0` such that

$$\sigma_\varepsilon^{\mathrm{low}} \geq \sigma_*.$$

A sufficient ledger is

$$a_\varepsilon^{\mathrm{sum}} \geq a_* > 0, \quad \nu_\varepsilon \geq \nu_* > 0, \quad \eta_\varepsilon \geq \eta_* > 0,$$

$$\kappa_\varepsilon^{\mathrm{wit}} \geq \kappa_* > 0, \quad b_\varepsilon^{\mathrm{cell}} \leq b^*, \quad r_\varepsilon^{\mathrm{bulk}} \leq r^*, \quad \ell_\varepsilon^+ \leq \ell^*,$$

with

$$a_*(\nu_* \eta_* \kappa_* - b^*) - r^* > 0.$$

UT2 - Uniform physical-length calibration. There exist `lambda_* > 0` and `c_*` such that

$$N_\varepsilon(R) \geq \lambda_* R - c_*.$$

UT3 - Refinement-neutral subdivision. Fine-cell subdivision changes the resolution, not the physical normalization class. It may not multiply the energy density by combinatorial bookkeeping.

UT4 - Uniform endpoint control.

$$\sup_{\varepsilon \in E_{\text{tail}}} C_\varepsilon^{\text{end}} < \infty.$$

Together these yield

$$\boxed{E_\varepsilon^{\text{rel}}(R) \geq \sigma_* R - C_*}$$

with constants independent of `epsilon` and `R`.

17.3 Scale-compatible relative renormalization

The transparent scalar subtraction must be compatible across the selected scale correspondences. A scale-dependent scalar drift independent of `R` is harmless for tension but may obstruct pointwise energy convergence; anchored potentials remove it.

No subtraction of two independently divergent bare branch energies is permitted.

17.4 Sector persistence

The selected scale correspondences must preserve, by independent source and target certificates,

$$q_- = -m, \qquad q_+ = m,$$

and the nontrivial bridge grade `m`.

The thin reconstruction must remain Type C:

- the pair and transparent packets survive;
- bounded local thin observables remain center neutral;
- isolated endpoints do not become new bounded vacuum objects;
- the nontrivial bridge sector does not enter the thin complete-ground kernel.

Forgetting the coefficient gerbe in a completion is not a physical proof that the charge vanished.

17.5 Thin relative energy

Let

$$E_0^{\text{rel}}(R) = E_0^{\text{pair}}(R) - E_0^0(R)$$

be the energy of the actual physically reconstructed thin dynamics.

The critical variational hypothesis is nonrelaxation:

$$\boxed{E_0^{\mathrm{rel}}(R) \geq \liminf_{n\to\infty} E_{\varepsilon_n}^{\mathrm{rel}}(R).}$$

A structural sufficient condition is constrained Mosco or equivalent variational convergence with:

1. compactness of bounded-energy pair-sector sequences;
2. preservation of the center-sector constraint;
3. admissible recovery sequences;
4. convergence of transparent scalar normalization;
5. no new thin zero-energy defect channel.

Ordinary lower semicontinuity without sector control is insufficient; the thin minimization could otherwise relax into a larger neutral category.

17.6 Theorem VF8.8

Assume G1-G5 hold on a cofinal positive-thickness tail, UT1-UT4 give the uniform bound, the relative renormalization and Type-C sector persist, the thin pair and transparent packets exist, and the thin constrained energy is nonrelaxing. Then

$$\boxed{E_0^{\mathrm{rel}}(R) \geq \sigma_* R - C_*.}$$

Consequently,

$$\boxed{\liminf_{R\to\infty} \frac{E_0^{\mathrm{rel}}(R)}{R} \geq \sigma_* > 0.}$$

The anchored thin potential satisfies the same lower asymptotic density.

If the thin energy is absolutely continuous, the thin restoring tension has Cesaro lower average at least `sigma_*`.

17.7 Order of limits

The clean construction is:

1. fix finite `R`;
2. perform admissible thin reconstruction;
3. obtain `E_0^{rel}(R)`;
4. then study `R -> infinity`.

The uniform lower bound also controls every admissible diagonal sequence, but equality or interchange of the thin and thermodynamic limits requires VF8.9.

17.8 G6 status

G6 closes only when both halves are proved:

$$\text{uniform positive-thickness density} \quad + \text{nonrelaxing physical thin reconstruction.}$$

One half without the other is a very respectable half theorem. It remains half a theorem.

18 VF8.9 - Uniform Finite-Block Almost-Additivity and the Thin Tension Limit

18.1 Why ordinary concatenation is wrong

Two physical Type-C pair states have boundary types

$$(-m, m) \quad \text{and} \quad (-m, m).$$

Naively placing them side by side produces four charged endpoints. That is not the desired composition and would use endpoint states that are not independently physical.

The correct operation fuses the middle charges

$$m \quad \text{and} \quad -m$$

through a fixed neutral interface correspondence. The middle charges are relative-boundary labels, not asymptotic physical objects.

18.2 Canonical physical blocks

Choose a mesoscopic physical block length

$$\Lambda > 0$$

independent of the ultraviolet subdivision and of `epsilon` on the cofinal tail.

Let

$$\mathcal{B}_\varepsilon^{[n]}$$

be the canonical `n`-block bridge with outer boundary type `(-m,m)` and physical separation

$$R_\varepsilon(n) = n\Lambda + \delta_\varepsilon(n), \qquad |\delta_\varepsilon(n)| \leq C_{\text{len}}.$$

Define the scalar relative block energy

$$\boxed{\mathcal{E}_{\varepsilon,m}(n) = E^{\mathrm{pair}}_{\varepsilon,m}(n) - E^{0}_{\varepsilon}(n).}$$

The pair and transparent blocks use the same interface and counterterm convention.

18.3 Neutral fusion

Require an admissible correspondence

$$\mathfrak{F}^{n,k}_{\varepsilon,m} : \mathfrak{P}^{[n]}_{\varepsilon,m} \boxtimes \mathfrak{I}_{\varepsilon,m} \boxtimes \mathfrak{P}^{[k]}_{\varepsilon,m} \rightsquigarrow \mathfrak{P}^{[n+k]}_{\varepsilon,m},$$

where the fixed-width interface packet `I` fuses the middle charges without adding matter, an external defect, or a new incision.

Scalar reassociators may compare different fusion orders. They act as unit-modulus coherence data and do not contribute an additive energy unless a separate dynamical coupling is proved.

18.4 Upper gluing estimate

Near-minimizing left and right block states yield a fused trial state. Require a uniform bound

$$\boxed{\mathcal{E}_{\varepsilon,m}(n+k) \le \mathcal{E}_{\varepsilon,m}(n) + \mathcal{E}_{\varepsilon,m}(k) + C_{\mathrm{glue}}.}$$

The constant is supported in one fixed interface star and is independent of `n`, `k`, and `epsilon` on the cofinal tail.

18.5 Lower cutting estimate

Cut an `(n+k)`-block state at a canonical interface. The induced cut faces carry opposite relative-boundary charges and are kept paired by a controlled cut correspondence. Require

$$\boxed{\mathcal{E}_{\varepsilon,m}(n+k) \ge \mathcal{E}_{\varepsilon,m}(n) + \mathcal{E}_{\varepsilon,m}(k) - C_{\mathrm{cut}}.}$$

No global tensor-product split is assumed. The cut constant contains only interactions and localization errors supported in one fixed-width interface neighborhood.

18.6 Uniform quasi-additivity

With

$$C_{\mathrm{aa}} = \max\{C_{\mathrm{glue}}, C_{\mathrm{cut}}\},$$

we obtain

$$\boxed{|\mathcal{E}_{\varepsilon,m}(n+k) - \mathcal{E}_{\varepsilon,m}(n) - \mathcal{E}_{\varepsilon,m}(k)| \le C_{\mathrm{aa}}.}$$

18.7 Homogenization lemma

Let `a(n)` satisfy

$$|a(n+k) - a(n) - a(k)| \le C$$

and a linear growth bound. Then

$$\tau = \lim_{n\to\infty} \frac{a(n)}{n}$$

exists and

$$\boxed{|a(n) - n\tau| \le C.}$$

The proof uses repeated fusion,

$$|a(qn) - qa(n)| \le (q-1)C,$$

followed by division with remainder `N=qn+r`. The finite-size error is uniformly bounded, not merely sublinear.

18.8 Positive-thickness block tension

Applying the lemma gives

$$\boxed{\tau_{\varepsilon,m} = \lim_{n\to\infty} \frac{\mathcal{E}_{\varepsilon,m}(n)}{n},}$$

and

$$|\mathcal{E}_{\varepsilon,m}(n) - n\tau_{\varepsilon,m}| \le C_{\mathrm{aa}}.$$

Define

$$\boxed{\sigma_{\varepsilon,m} = \frac{\tau_{\varepsilon,m}}{\Lambda}.}$$

The G6 lower bound implies

$$\sigma_{\varepsilon,m} \geq \sigma_* > 0.$$

A uniform terminal-block estimate comparing arbitrary `R` with the nearest canonical block length then gives

$$\lim_{R\to\infty} \frac{E^{\mathrm{rel}}_{\varepsilon,m}(R)}{R} = \sigma_{\varepsilon,m}.$$

18.9 Thin finite blocks

Require fixed-block variational convergence:

$$\boxed{\mathcal{E}_{\varepsilon,m}(n) \longrightarrow \mathcal{E}_{0,m}(n)}$$

for every fixed `n`, preserving boundary type, center sector, and relative normalization.

Uniform quasi-additivity passes to the limit:

$$|\mathcal{E}_{0,m}(n+k) - \mathcal{E}_{0,m}(n) - \mathcal{E}_{0,m}(k)| \leq C_{\mathrm{aa}}.$$

Hence

$$\boxed{\tau_{0,m} = \lim_{n\to\infty} \frac{\mathcal{E}_{0,m}(n)}{n}}$$

exists, with

$$|\mathcal{E}_{0,m}(n) - n\tau_{0,m}| \leq C_{\mathrm{aa}}.$$

Define

$$\boxed{\sigma_{0,m} = \frac{\tau_{0,m}}{\Lambda} \geq \sigma_* > 0.}$$

18.10 Convergence of regulated tensions

The uniform finite-size estimate gives

$$|\tau_{\varepsilon,m} - \tau_{0,m}| \leq \frac{2C_{\mathrm{aa}}}{n} + \frac{1}{n}|\mathcal{E}_{\varepsilon,m}(n) - \mathcal{E}_{0,m}(n)|.$$

First take `epsilon -> 0` at fixed `n`, then `n -> infinity`. Thus

$$\boxed{\tau_{\varepsilon,m} \to \tau_{0,m}, \qquad \sigma_{\varepsilon,m} \to \sigma_{0,m}.}$$

For canonical finite blocks, the thin and thermodynamic limits commute.

18.11 Full thin separation limit

A thin terminal-block interpolation estimate yields

$$\boxed{\lim_{R\to\infty} \frac{E^{\mathrm{rel}}_{0,m}(R)}{R} = \sigma_{0,m} > 0.}$$

Moreover,

$$E^{\mathrm{rel}}_{0,m}(R) = \sigma_{0,m}R + O(1).$$

If the thin energy is absolutely continuous, the restoring tension has exact Cesaro limit `sigma_0,m`. Pointwise force convergence still requires derivative control of the bounded remainder.

18.12 Orientation symmetry

The `m=1` and `m=2` branches are opposite orientations. Equality

$$\sigma_{0,1} = \sigma_{0,2}$$

requires a charge-conjugation correspondence preserving the Hamiltonian, block geometry, transparent reference, and interface convention. Without that proof, retain two separately labeled positive tensions.

18.13 Theorem VF8.9

Uniform neutral fusion, controlled cutting, fixed-block thin convergence, and terminal-block interpolation close G7. They produce an actual positive thin tension limit rather than only a positive lower asymptotic density.

19 VF8.10 - Combined Theorem, Dependency Graph, and Claim-Boundary Audit

19.1 Logical status

Every statement in the VF8 architecture has one of four statuses:

- **R - retained input:** already supplied by the controlling positive-thickness manuscript;
- **C - constructed theorem schema:** typed objects, hypotheses, and proof architecture supplied here;
- **O - open verification obligation:** a bridge-specific hypothesis not yet proved;
- **X - excluded claim:** a conclusion that does not follow even if G1-G7 close.

A conditional theorem is not a slogan. It has explicit objects, assumptions, conclusions, proof steps, and failure modes. Its unresolved status lies in verifying those assumptions in the actual bridge model.

19.2 Retained inputs

The controlling positive-thickness package supplies:

1. the selected source-free Sector-III `SU(3)` branch;
2. nontrivial classes $[\widehat{\Omega}_m]_{\text{phys}}$, $m = 1, 2$, with $I_3(\widehat{\Omega}_m) = \omega^m$;
3. honest triality and compatible Gauss-Ward data;
4. zero finite current defect;
5. the complete-ground projection;
6. the uniform positive-thickness coercive estimate

$$\overline{q}_x \geq \kappa_{\text{cof}}(I - P_{\Omega,x}), \qquad \kappa_{\text{cof}} = 0.337404437602020\ldots;$$

7. selected regional, chart, Cauchy, stackification, and scale transport;
8. the explicit exclusion of thin reconstruction, confinement, scattering, and mass-gap claims from Paper III.

19.3 Dependency graph

The recommended proof order is

$$\boxed{G1 \longrightarrow G2 \longrightarrow G3 \longrightarrow G5 \longrightarrow G4 \longrightarrow G6 \longrightarrow G7.}$$

G5 is audited before final closure of G4 because one must first decide which seam and collar terms are truly `O(1)` and which are repeated bulk losses.

The PDF contains the same graph as a typeset figure.

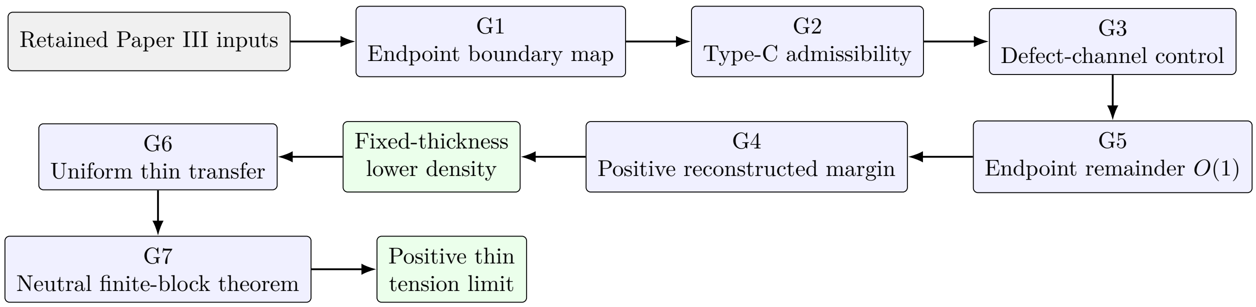

Figure 1: Dependency graph for the VF8 verification gates. The ordering places the endpoint audit before the final reconstructed-margin claim so repeated seam losses cannot be hidden in an $O(1)$ remainder.

19.4 Gate ledger

Gate	Required conclusion	Architecture	Verification
G1	$q_- = -q_+ \neq 0$	VF8.1	Open
G2	Pair and transparent physical; isolated endpoints excluded	VF8.2–VF8.3	Open
G3	Full bridge defect lies in the coercive complement	VF8.4	Open
G4	$\Delta_\varepsilon^{\mathrm{norm}} > 0$ after all bulk losses	VF8.5	Open
G5	Uniform $O(1)$ endpoint remainder	VF8.6	Open
G6	Positive density survives physical thin reconstruction	VF8.8	Open
G7	Uniform quasi-additivity and exact thin tension limit	VF8.9	Open

The theorem architecture is complete. The verification status remains zero fully discharged gates. Writing the theorem one needs is not the same thing as proving the hypotheses it needs. This distinction is the note's main act of self-defense.

19.5 Master conditional theorem

Let $m \in \{1, 2\}$. Assume the retained positive-thickness inputs and verify G1-G7 along an admissible cofinal thickness system. Then:

1. the coefficient detector is physically realized as
$$m[\mathcal{B}_{\varepsilon,R}];$$
2. the endpoint charges are
$$q_- = -m, \qquad q_+ = m;$$
3. the endpoint system is Type C;

4. the pair-versus-transparent relative energy is the only admissible connected vacuum comparison;
5. every bridge cell occupies a nontrivial detector channel controlled by the complete-ground complement;
6. bounded-overlap reconstruction yields a positive fixed-thickness spatial density;
7. endpoint contributions remain `O(1)`;
8. the density survives admissible thin reconstruction;
9. finite-block energies are uniformly quasi-additive;
10. the thin tension exists and is positive:

$$\boxed{\lim_{R\to\infty} \frac{E^{\mathrm{rel}}_{0,m}(R)}{R} = \sigma_{0,m} > 0.}$$

Moreover,

$$E^{\mathrm{rel}}_{0,m}(R) = \sigma_{0,m} R + O(1),$$

and, under absolute continuity, the restoring tension has Cesaro limit `sigma_0,m`.

19.6 Proof skeleton

The complete proof would proceed as follows.

1. Extract the discrete grade using `I_3`.
2. Transgress the meridional character to the transverse Thom class.
3. Apply Poincare-Lefschetz duality to obtain the longitudinal bridge class.
4. Take its relative boundary to obtain opposite endpoint charges.
5. Prove the exponentiated center Gauss-Ward balance.
6. Prove bounded local vacuum operations preserve triality.
7. Construct finite-energy pair and transparent states.
8. Identify the nontrivial bridge projector with the complete-ground complement.
9. Apply local coercivity to the full defect channel.
10. Reconstruct the global bridge lower bound by bounded overlap.
11. Prove only two endpoint stars and two attachment seams remain `O(1)`.
12. Establish a uniform cofinal density and nonrelaxing thin form convergence.
13. Fuse and cut neutral finite blocks with a uniform interface defect.
14. Homogenize the quasi-additive block energies.

19.7 What each failed gate means

- If **G1** fails, the coefficient class remains nontrivial but no separated endpoint pair is certified.
- If **G2** fails, isolated endpoints or other dressings may be physical and the pair-only subtraction is invalid.
- If **G3** fails, the bridge sector may intersect the complete-ground kernel.
- If **G4** fails, seam or reconstruction losses overwhelm the local gap.

- If **G5** fails, an allegedly local endpoint term may grow with separation.
- If **G6** fails, positive density may collapse in the thin theory.
- If **G7** fails, the strongest conclusion is a positive liminf density, not an exact tension limit.

19.8 Historical and interpretive claim

The note may claim that QFT repeatedly displayed the structural ingredients later organized by gerbes:

- local data glued through projective or correspondence-valued comparisons;
- charged representations beyond the strict observable shadow;
- extended operators detecting linked center flux;
- boundary balance not reducible to local Lie-algebra charge;
- coherent higher cocycles surviving changes of presentation.

It should not claim that early authors secretly wrote bundle-gerbe theory, nor that Wilson lines, superselection sectors, or projective implementers are newly discovered here. The contribution is the typed recasting and the theorem architecture connecting those ingredients.

19.9 Precise confinement terminology

If G1-G7 close, the result is:

> Linear pair-separation energy in the selected source-free Type-C `SU(3)` center sector under admissible thin reconstruction.

The word *confinement* should always carry that scope. The result would not automatically cover every representation, every boundary condition, every charge type, or every gauge-group global form.

19.10 Explicit nonclaims

Even full G1-G7 closure would not by itself prove:

- a vacuum spectral mass gap for all local excitations;
- an area law for every Wilson observable;
- scattering or asymptotic completeness;
- Wightman or Osterwalder-Schrader reconstruction;
- pointwise force convergence;
- unrestricted descent over arbitrary scales, charts, or Cauchy slices.

19.11 Honest present status

At version 0.2.1,

VF8.1–VF8.10 provide a complete conditional architecture, while G1–G7 remain open verification gates.

The retained manuscript does not already contain these bridge proofs. The note remains a research note, not a completed confinement paper.

That is not a demotion. Notes preserve the shape of an idea before journal compression removes the fingerprints. They are also where one is allowed to say, plainly, that a nontrivial gerbe class is an obstruction certificate, not an energy estimate. The Hamiltonian still has to do some work. Mathematics remains stubborn that way.

20 References and Historical Landmarks

The references below are landmarks rather than an exhaustive history. They do not all use the same formal language or make the same physical claims. The historical thesis is structural: these works exhibit extended flux, operator algebras, sector data, projective or higher-cohomological geometry, and local-to-global obstruction.

1. K. G. Wilson, *Confinement of Quarks*, Physical Review D **10** (1974), 2445-2459.
2. J. Kogut and L. Susskind, *Hamiltonian Formulation of Wilson's Lattice Gauge Theories*, Physical Review D **11** (1975), 395-408.
3. G. 't Hooft, *On the Phase Transition Towards Permanent Quark Confinement*, Nuclear Physics B **138** (1978), 1-25.
4. R. Haag, *Local Quantum Physics: Fields, Particles, Algebras*, second edition, Springer, 1996.
5. J.-L. Brylinski, *Loop Spaces, Characteristic Classes and Geometric Quantization*, Progress in Mathematics 107, Birkhauser, 1993.
6. M. K. Murray, *Bundle Gerbes*, Journal of the London Mathematical Society **54** (1996), 403-416.
7. D. S. Freed, *Dirac Charge Quantization and Generalized Differential Cohomology*, arXiv:hep-th/0011220, 2000.